RESEARCH ARTICLE

A Selective Study on Decolorization of Textile Azo Dye using Genetically Modified Brown-Rot Fungi

Manikandan Dhashanamoorthy[1], S. Chacko Vijai Sharma[2]*

Department of Microbiology, K. M. G. College of Art and Science, Vellore, Tamil Nadu, India

ABSTRACT

Aim: Bioremediation of textile effluents using microorganisms can transfer toxic dyestuffs into non-toxic. Moreover, the discovery of the value of brown-rot fungi in bioremediation has brought a great success in this field. Molecular biology related to brown-rot fungi, especially related to the extraction of genetic material (RNA and DNA), gene cloning, and the construction of genetically engineered microorganisms is especially attractive and thus investigated in recent years. Steam-assisted dry gel conversion of tetraethyl orthosilicate and sodium aluminate to ZSM-5 and ZSM-5 activated carbon composite. **Result:** The resulting material exhibited hierarchical pore structure with high surface area and porosity as characterized by X-ray diffraction and nitrogen adsorption. The addition of activated carbon enhanced the surface area and adsorption percentage of aqueous lead (Pb^{2+}) and cadmium (Cd^{2+}) from aqueous solution and further from industrial effluents. **Conclusion:** The co-ordination of the alumina incorporated was analyzed using Al magic-angle spinning nuclear magnetic resonance. ZSM-5/activated carbon composite with high crystallinity was obtained which exhibited high adsorption rates when compared to ZSM-5, activated carbon individually, and their mechanical mixtures.

Keywords: Brown-rot fungi, decolorization of textile dye, genetically modified

INTRODUCTION

The designation "brown-rot fungi" refers to the members of the basidiomycetes, a class of fungi that degrade lignin more rapidly than carbohydrates during the decay of wood under aerobic conditions. As the colored lignin pigments are degraded, the decaying wood acquires a white appearance. During early development, the filamentous organisms consist of undifferentiated, non-pigmented generative hyphae that grow through cell enlargement and tip extension before developing into specialized hyphae. An ecological advantage of fungi over bacteria pertains to their ability to secrete enzymes into the environment from the growing tips of their filamentous

hyphae. Various basidiomycetous species have been investigated for their capacity to produce ligninolytic enzymes within industrial processes or for the treatment of contaminated effluents, soil, or aquifers.[1] *Phanerochaete chrysosporium, Trametes versicolor,* and *Bjerkander* species frequently surpass other fungi through the effectiveness of the enzymes that they produce. Consequently, they are among the well studied of the organisms that produce ligninolytic enzymes. However, various strains of these species produce diverse types and quantities of ligninolytic enzymes depending on the culture medium and environmental conditions. The influential factors for enzyme production are nutrient availability, oxygen concentration, temperature, pH, agitation, and culture medium.[2] Brown-rot fungi break down the lignin in wood, leaving the lighter-colored cellulose behind. Some of them break down both lignin and cellulose. Because brown-rot fungi are

---

*Corresponding Author:
Dr. S. Chacko Vijai Sharma,
E-mail: chackosd1614@gmail.com

able to produce enzymes, such as laccase, needed to break down lignin and other complex organic molecules; they have been investigated for use in mycoremediation applications. Fungi from the basidiomycetous group, are known as brown-rot fungi, are heterogeneous group of microorganisms but have in common the capacity to degrade lignin as well as other wood components. The brown-rot fungi are by far the most efficient ligninolytic microorganisms. They are able to degrade a wide variety of recalcitrant pollutants including various types of dyes. Most information on the biodegradation of synthetic dyes by ligninolytic fungi have been obtained with *P. chrysosporium*. Brown-rot fungus showed some capacities to remove dyes from industrial effluents. The fungus has been studied for their ability to degrade recalcitrant organic pollutants such as polyaromatic hydrocarbons, chlorophenols, and polychlorinated biphenyl. The decolorization of phenol red, methylene blue, Coomassie blue, dextran blue etc., has been used to indicate ligninolytic activity.[3] However, the main characteristic that differentiates brown-rot fungi from most other microorganisms is their ability to completely mineralize all components of lignin to carbon dioxide and water.[4] Besides the role in wood degradation brown-rot fungi can be applied for degradation of different industrial contaminants such as low molecular polycyclic aromatic carbohydrates, aromatic carbohydrate, and chlorophenol.[5] Disposal of untreated effluent to the surroundings often leads to the following consequences, (a) makes the water bodies colored and creates esthetic problem, (b) limits the reoxygenation capacity of the receiving water and cuts-off sunlight which in turn disturbs the photosynthetic activities in the aquatic system, and (c) causes chronic and acute toxicity. Thus, it is mandatory to treat dye bath effluents before discharge into the surrounding aquatic systems.[6] The textile industries utilize large volumes of water in its processing operations and generate substantial quantities of wastewater. Dye wastes are usually discarded into water with or without processing. Aesthetic merit, gas solubility, and water transparencies are affected by the presence of dyes even in small amounts.[7] All dyes used in the textile industry are designed to resist fading upon exposure to sweat, light, water, many chemicals including oxidizing agents, and microbial attack. During processing, up to 15% of the used dyestuffs are released into the process water. Dye-containing effluents are hardly decolorized by conventional biological wastewater treatments. In addition to their visual effect and their adverse impact in terms of chemical oxygen demand, many synthetic dyes are toxic, mutagenic, and carcinogenic. Most of these enzymes are industrially important and have the great potential in processes of bioremediation, biodegradation, biopulping, and degradation detoxification of recalcitrant substances.[8-11] The most common ligninolytic peroxidases produced by almost all brown-rot basidiomycetes and by various litter-decomposing fungi are manganese peroxidases. These are glycosylated glycoproteins with an iron protoporphyrin IX (heme) prosthetic group, molecular weights between 32 and 62.5 kDa and are secreted in multiple isoforms.

MATERIALS AND METHODS

Chemicals

All chemicals were of analytical grade purchased from Qualigens fine chemicals, India, SRL, India, Sigma chemical co, USA, and E Merck Ltd., India. Antibiotics, media, and agar powder were purchased from Hi-media Laboratories Pvt. Ltd., India.

Collection of samples from various geographical areas

Sample collection containers, forceps, markers, and hand clove.

Spore suspension preparation

Potato dextrose broth and conical flasks.

Lacto phenol cotton blue staining

Lactophenol cotton blue, glass slide, coverslips, and petroleum jelly.

Isolation of brown-rot fungi

- Potato dextrose agar – 3.9 g
- Chloramphenicol – 0.01%
- Benomyl – 1%.

Screening of laccase producers

- Potato dextrose agar – 3.9 g
- Guayacol – 0.01%.

Preservation and maintenance

Potato dextrose agar and test tubes.

Reagents for assay of laccase enzyme

Phosphate buffer preparation
- Disodium hydrogen phosphate – 8.954 g
- Potassium dihydrogen phosphate – 3.4023 g

Dissolve 8.954 g of disodium hydrogen phosphate and 3.4023 g of potassium dihydrogen phosphate in 1 l of distilled water.
- Phosphate buffer – 0.1 M (pH-4.5)
- Guayacol – 0.5 ml.

Collection of commercial dyes and chemicals

Sterile sample containers, spatula, and cloves.

Decolorization assay use of minimal media

Yeast extract, glucose, minerals, tween 20, wheat bran, and Erlenmeyer flask.

Materials for decolorization of textile dye effluent

Medium: Potato dextrose broth.

Reagents for estimation for laccase by Lowry's method

Solution 1: Alkaline copper reagent
- 2 g of sodium carbonate was dissolved in 100 ml of 0.1N NaOH.

Solution 2: Copper sulfate solution
- Dissolve 0.5% of copper sulfate in 1% sodium potassium tartrate.
Reagent A:
- 50 ml of solution 1 was mixed with 1 ml of solution 2.
Reagent B:
- 1:2 dilution of commercial Folin–Ciocalteu reagent.
Solution 6: Standard protein – Bovine serum albumin (BSA)
- Dissolve 10 mg of BSA in 10 ml of double distilled water.
Solution 7: Working standard
- Makeup 1 ml of stock standard to 10 ml. It gives 100 µg/ml concentration.

Mutagenesis study using ultraviolet (UV)

- Brown-rot fungi
- UV chamber
- Potato Dextrose agar plates
- Dark clothes.

RESULTS AND DISCUSSION

The ZSM-5/AC composite, ZSM-5, and mechanical mixture (MM) were prepared to assess the effect of activation and the changes in the physical characteristics of the resulting adsorbents. The intercalation of H_3PO_4 in the carbon matrix and the steam-assisted dry gel conversion (SADGC) [Figure 1], method for the composite preparation results in the formation of new micropores, which increases the surface area and porosity, was observed from the Brunauer–Emmett–Teller (BET) analysis. However, the adsorption capacities of Pb^{2+} and Cd^{2+} by the ZSM-5/AC composite were considerably high in comparison with ZSM-5 and the MM.

X-ray diffraction (XRD) analysis of the prepared sorbents

Although the preparation of the ZSM-5/AC composite was carried out under basic conditions, no significant change was observed in Si or Al content in ZSM-5 and ZSM-5/AC composite.

Thus, the ZSM-5 and the ZSM-5/AC composite have active sites which are principally located in the structure channels and also on the external surface of the crystallites.[12,13] XRD patterns of the ZSM-5, ZSM-5/AC composite, and the MM are shown in Figure 2.

No crystalline phase was observed in AC when compared with ZSM-5/AC, ZSM-5, and MM which was crystalline which also agrees well with the reported literature. It appears, therefore, that there is no drastic change in the crystal chemistry of the ZSM-5 samples before and after composite formation. A general slight decrease of the diffraction peak intensity is observed for all the crystalline phases which were more pronounced for ZSM-5/AC composite. The data obtained composed with a conventional diffractometer, down with the polycrystalline nature of the samples, did not allow obtaining an elevated excellence in structure refinement of ZSM-5/AC composite aimed to prove the change in the extra-framework population between the ZSM-5 and ZSM-5/AC composite, respectively.[14]

Scanning electron microscope (SEM) analysis of prepared sorbents

The SEM micrographs of ZSM-5/AC and ZSM-5 sample are presented in Figure 3a and b. Except in activated carbon, crystalline zeolite particles are visible in all other samples. SEM micrographs of the ZSM-5 and ZSM-5/AC composite crystals show a tabular morphology of the crystals of ZSM-5.[15-18] Form and size of the crystallites are preserved despite the basic composition of the composite [Figure 3c and d].

Al magic-angle spinning (MAS) nuclear magnetic resonance (NMR) and Fourier-transform infrared (FTIR) of prepared sorbents

Further structural configuration of Al atoms was investigated by Al-MAS NMR shown in Figure 4. A pronounced peak at around 56 ppm can be seen
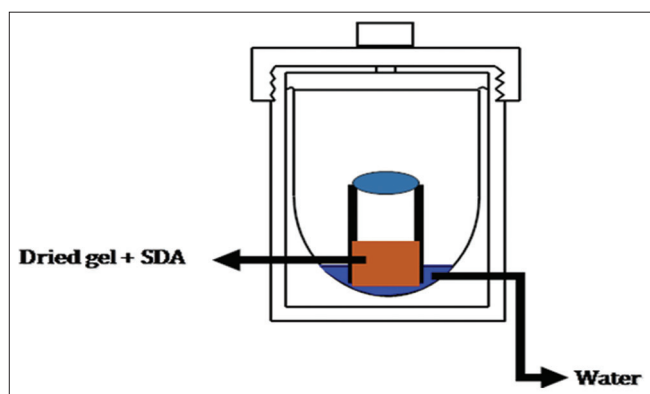

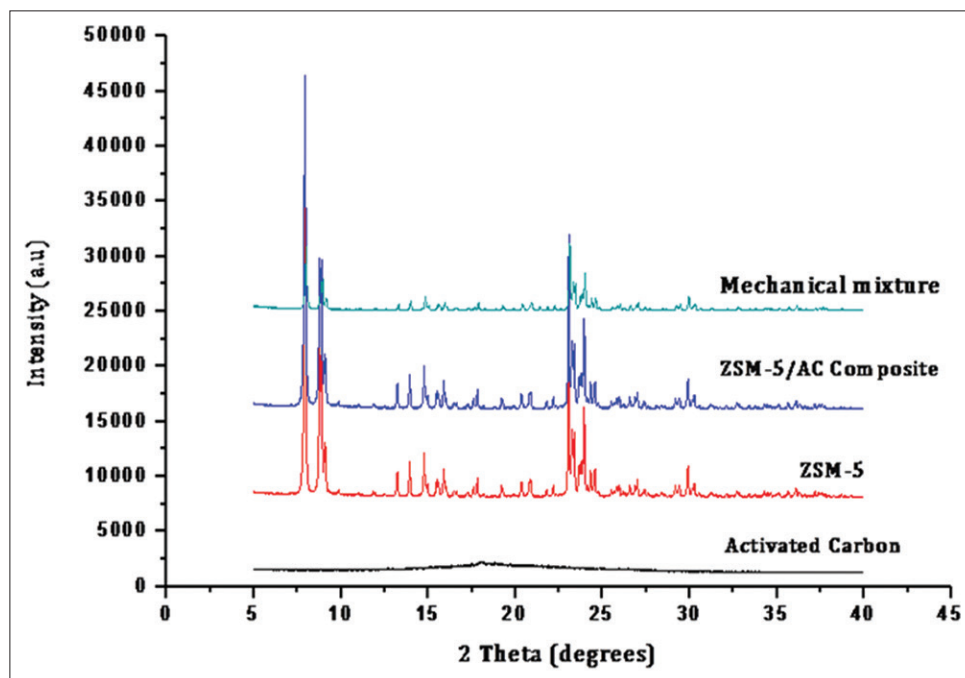**Figure 1:** Set up of steam-assisted dry gel conversion

Figure 2: X-ray diffraction patterns of activated carbon ZSM-5 with Si/Al ratio of 25, ZSM/AC
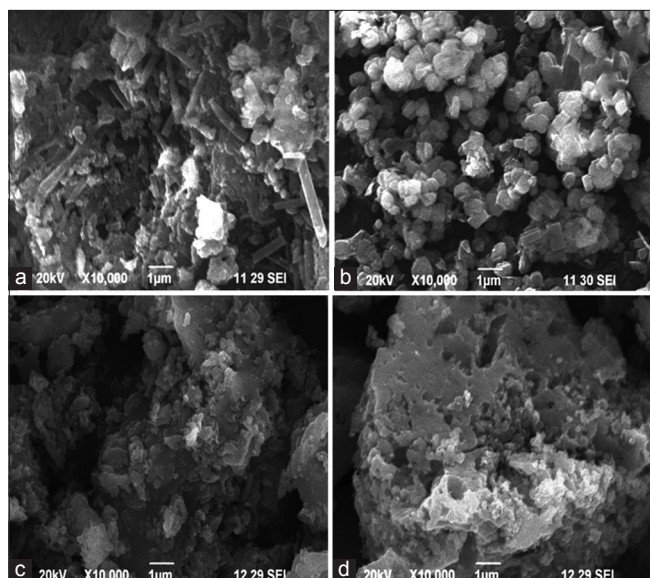
Figure 3: (a) Scanning electron microscope (SEM) micrographs of AC; (b) SEM micrographs of ZSM-5; (c) SEM micrographs of mechanical mixture; (d) SEM micrographs of ZSM-5/AC
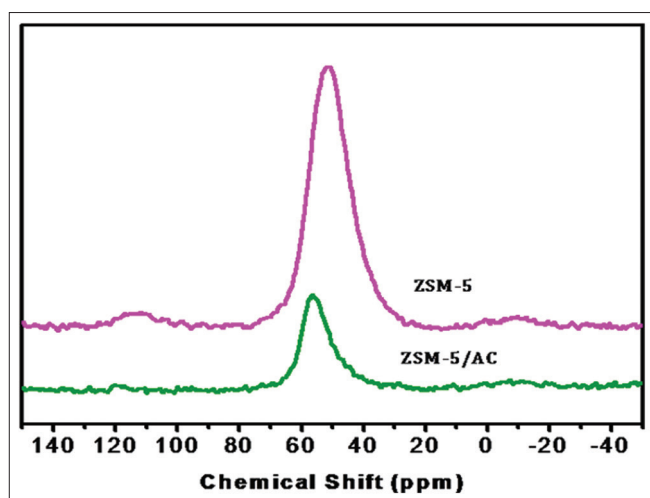

Figure 4: Al magic-angle spinning nuclear magnetic resonance of ZSM-5 and ZSM-5/AC-+

both in the ZSM-5 and ZSM-5/AC. It corresponds to tetrahedral geometry of the alumina. The absence of a peak at 0 ppm indicates clearly that Al is entirely incorporated in the framework of both ZSM-5 and ZSM-5/AC.[19] The FTIR spectra are shown in Figure 5, and significant ring structure of silica and the double 5 ring of crystalline ZSM-5 can be clearly seen and the same is presented in Table 1.

Surface area of prepared sorbents using BET

The characteristics of ZSM-5, ZSM-5/AC, and MM prepared at optimum conditions were determined

Table 1: FT-IR of ZSM-5, ZSM-5/AC, and MM

Wavenumber (cm^{-1})			Functional group
ZSM-5	ZSM-5/AC	MM	
800	800	734	Ring structure of silica
547	549	550	Double 5 rings of crystalline ZSM-5

FT-IR: Fourier-transform infrared, MM: Mechanical mixture

Table 2: Characteristics of the prepared adsorbents

Physical properties	ZSM-5	ZSM-5/AC	MM
Surface area (m^2/g)	877.25	1296	956.4
Total pore volume (cc/g)	9.4	4.2	7.4
BJH average pore diameter (nm)	4.4	2.5	4.6

MM: Mechanical mixture

by BET analysis, and date is summarized in Table 2. These results show that the surface areas of ZSM-5, ZSM-5/AC, and MM were 877.25, 1296, and 956.4 m^2/g, respectively. The high surface area of ZSM-5/AC helps in maximum Pb^{2+} and Cd^{2+} uptake when compared with ZSM-5 and MM. These micropores are preferable for adsorption of Pb^{2+} and Cd^{2+} ions since these ions also have smaller ionic radii similar to that of the micropores formed by ZSM-5/AC.[20-23]

Batch mode adsorption studies

Effect of pH on adsorption

The effect of pH on the process of adsorption is of great importance since it influences chemical speciation of the metal in solution and also on the ionization of chemically active sites on the sorbent surface. The pH at which sorbent surface charge takes a zero value is defined as the point of zero charge (pHpzc). The knowledge of pHpzc allows one to get some knowledge on the ionization of functional groups at the sorbent surface and their interactions with metal species in solution; at pHs higher than pHpzc, sorbent surface is negatively charged and could interact with metal species, while at pHs lower than pHpzc, solid surface is positively charged and could interact with negative species. The obtained pHpzc of ZSM-5/AC was pH 6 ± 0.1 while pHpzc was 5.5 ± 0.1 for the ZSM-5. This important and crucial parameter for batch adsorption process was studied, as it affects the surface charge of the adsorbents and the degree of ionization of adsorbate during adsorption
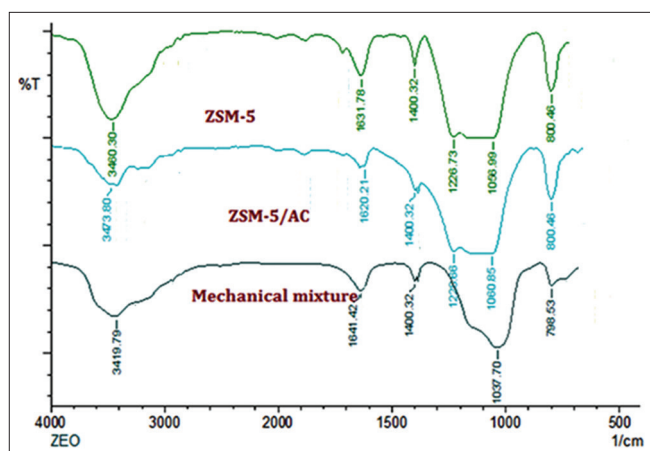
Figure 5: Fourier-transform infrared of ZSM-5, ZSM-5/AC, and mechanical mixture

Table 3: Effect of pH on the removal of Pb²⁺ and Cd²⁺

| pH | Removal % of ions by | | | | | |
| | ZSM-5/AC% | | MM | | ZSM-5 | |
	Pb²⁺	Cd²⁺	Pb²⁺	Cd²⁺	Pb²⁺	Cd²⁺
2	54.56	52.5	51.23	57.18	66.54	68.22
3	65.5	65.30	65.8	61.45	72.45	72.21
4	69.78	74.58	69.51	69.78	82.12	81.81
5	98.56	96.34	77.13	73.44	88.62	86.40
6	91.45	89.65	95.78	95.65	97.18	96.15
7	85.34	76.45	92.12	91.10	93.90	88.95

MM: Mechanical mixture

process. pH influences metal ion sorption due to the competition between metal ions and H⁺ ions for active sorption sites, and hence, the effect of H⁺ ion concentration on removal of Pb²⁺ and Cd²⁺ by ZSM-5, ZSM-5/AC, and MM was studied at different pH ranging from 2 to 7 [Table 3]. It could be observed that adsorption of Pb²⁺ and Cd²⁺ increases as the pH increased from 2 to 6. Beyond pH 6, the removal efficiency was found to decrease for both the adsorbents. Similar observations were reported for removal of Cd²⁺ ions by watermelon rind. Hence, further sorption experiments were carried out at pH 6 for ZSM-5, ZSM-5/AC, and MM.[24,25]

Kinetics of adsorption

Kinetics of the adsorption process was studied for all the three adsorbent with respect to contact time. Sorption experiments were conducted at different time intervals (10–120 min) for removal of Pb²⁺ and Cd²⁺ ions onto ZSM-5, ZSM-5/AC, and MM. The uptake of Pb²⁺ and Cd²⁺ was rapid initially, and equilibrium had been achieved within 60 min. To analyze the mechanism and rate of adsorption of Pb²⁺ and Cd²⁺ ions onto prepared sorbents, experimental data were fitted to pseudo first-order and pseudo second-order models.

Pseudo first-order kinetic model
The linear form of pseudo first-order equation is given as,

$$\ln(q_e - q_t) = \ln q_e - k_1 t \qquad (1)$$

q_e is the amount of metal adsorbed at equilibrium (mg/g), q_t is the amount of metal adsorbed at time t, and k_1 is the first-order reaction rate constant. The theoretical (q_e) values found from the pseudo first-order kinetic model calculated from Eq. 1 were observed to have large difference compared to experimental values, and further, the low correlation coefficients (R^2) also suggest a poor pseudo first-order fit of the experimental data.

Pseudo second-order kinetic model
The kinetic data were also analyzed using pseudo second-order kinetic model as per Eq. 2. Equilibrium capacity of pseudo second-order model is shown in Table 4. Pseudo second-order kinetics for Pb²⁺ and Cd²⁺ parameters with experimental values obtained at 30°C is given. The values and correlation coefficients (R^2) for pseudo second-order model are also represented. It was observed that the theoretical q_e values were very close.

$$\frac{t}{q_t} = \frac{1}{k_2 q_e^1} + \frac{t}{q_e} \qquad (2)$$

These observations suggest that sorption by ZSM-5, ZSM-5/AC, and MM follows pseudo second-order kinetic reaction, which suggests that the process controlling the rate may be a chemical sorption involving valence forces through sharing or exchanging of electrons between adsorbate and adsorbent.

In general, the experimental data that fit to pseudo second-order model indicate that the rate-limiting step for the process involves chemical reaction, i.e. chemisorption. A number of conditions must be met if the rate of removal of heavy metals from

Table 4: Pseudo first- and second-order kinetic data for Pb^{2+} and Cd^{2+} parameters with experimental values obtained at 30°C

Model	Constants	ZSM-5/AC		ZSM-5		MM	
		Pb^{2+}	Cd^{2+}	Pb^{2+}	Cd^{2+}	Pb^{2+}	Cd^{2+}
Experimental	q_e (mg/g)	118.56	105.41	105.4	101.14	95.10	78.26
Pseudo first order	q_e (mg/g)	61.71	51.35	41.53	39.35	43.51	38.89
	k_1 (min^{-1})	0.081	0.091	0.031	0.059	0.032	0.045
	R^2	0.956	0.917	0.915	0.952	0.955	0.993
Pseudo second order	q_e (mg/g)	105.25	101.15	101.15	99.83	91.54	71.59
	k_2 (g/mg/min)	0.015	0.012	0.062	0.056	0.075	0.035
	R^2	0.999	0.999	0.998	0.999	0.998	0.999

MM: Mechanical mixture

solution is controlled by chemical reactions. These conditions are,

- The rate constant should be constant for all values of initial concentration of counterions,
- The rate constant should not change with adsorbent particle size, and
- The rate constant is sometimes independent of the degree of agitation (stirring rate).

If any of these conditions is not satisfied, chemical reaction kinetics is not rate controlling even if the rate data are successfully fitted to pseudo second-order model.[26] To test whether the rate of removal of Pb^{2+} and Cd^{2+} ions is controlled by reactions, kinetic experiments were conducted at two different initial metal ion concentrations. From Table 4a and b, it is seen that rate constant k, for the removal of Pb^{2+} and Cd^{2+} ions, was not constant for different initial metal ion concentrations. This lack of consistency in the rate constants is proof that even though the results provide an excellent fit to the pseudo second-order kinetic model, the rate limiting step is not chemisorptions.

Adsorption isotherms

Evaluation of the maximum loading capacity of ZSM-5, ZSM-5/AC, and MM was carried out through sorption experiments conducted at different initial metal ion concentrations (50–300 mg/L) of Pb^{2+} and Cd^{2+} ions at equilibrium.

Langmuir isotherm

The Langmuir isotherm assumes monolayer adsorption process, and linear form of Langmuir isotherm after rearrangement is given as,

$$\frac{c_e}{q_e} = \frac{1}{bV_m} + \frac{C_e}{V_m}$$

(3)

Where C_e is the concentration of metal solution at equilibrium (mg^{-1}), q_e is the amount of metal adsorbed per unit mass of adsorbent (mg/g), V_m is the amount of adsorbate at complete monolayer coverage (mg/g), and b is a constant that relates to the heat of adsorption (L/mg). The maximum uptake of Pb^{2+} and Cd^{2+} by ZSM-5/AC, ZSM-5, and MM prepared at optimum conditions calculated from Eq. 3. The calculated constants of Langmuir isotherm equation for the two samples along with R^2 values are presented in Table 5. This table shows the maximum uptake of Pb^{2+} and Cd^{2+} by ZSM-5, ZSM-5/AC, and MM mixture. The uptake of Pb^{2+} and Cd^{2+} of ZSM-5/AC at a given metal ion concentration is higher than that of ZSM-5, MM, and AC which may be due to the high surface area exhibited by ZSM-5/AC through SADGC and may be due to the ability of ZSM-5/AC to produce highly microporous structure as compared to that ZSM-5 and MM.

Removal of Pb^{2+} and Cd^{2+} from industrial effluent

In an effort to examine the practical utility of prepared ZSM-5, ZSM-5/A, and MM out to remove Pb^{2+} and Cd^{2+} from the industrial effluent after optimizing conditions of Pb^{2+} and Cd^{2+} removal from aqueous solution, effluent samples collected from industrial areas of Vellore district were tried out for removal of the two metal ions. The collected effluent was filtered to remove all

the insoluble portions, and the filtrate was taken for study. The Pb^{2+} and Cd^{2+} concentration in the effluent was measured to be 25.5 and 21.3 mg/L, and the pH of the effluent was 1.5 [Table 6]. For the treatment of this effluent by ZSM-5, ZSM-5/AC, and MM, the optimized condition was used. It can be observed that approximately 98% and 90% of Pb^{2+} and Cd^{2+} by ZSM-5/AC; 92% and 90% of Pb^{2+} and Cd^{2+} by ZSM/5; and 80% and 88% of Pb^{2+} and Cd^{2+} by MM. Since the prepared adsorbents are biodegradable, it can be easily disposed after recovering Pb^{2+} and Cd^{2+} from the biosorbent by desorption.

Removal of Pb^{2+} and Cd^{2+} in the presence of other bivalent metal ions

The effect of other bivalent metals in the removal of Pb^{2+} was studied, and the data are reported in Table 7. The data suggest that there was a marginal decrease of 1–3% in the presence of Cu^{2+}, Zn^{2+}, and Co^{2+}. In the presence of Cd^{2+}, the decrease noticed was 9%, and in the multiple metal system, 8.9% was noticed. This proves that the sorbents had preferential adsorption of Pb^{2+} ions and no significant decrease in the sorption with the interferences of other metal ions. The other bivalent metal ions role in the removal of Cd^{2+} ions was studied, and the data are reported in Table 8. As observed from the data, 2–8% decrease was noticed in the sorption of Cd^{2+} in the presence of Cu^{2+}, Zn^{2+}, and Co^{2+} ions. In the presence of Pb^{2+}

Table 5: Pb^{2+} and Cd^{2+} equilibrium isotherm results

Sample	q_m (mg/g)		B (l/mg)		R^2	
	Pb^{2+}	Cd^{2+}	Pb^{2+}	Cd^{2+}	Pb^{2+}	Cd^{2+}
ZSM/AC	131.55	121.24	0.341	0.213	0.999	0.999
ZSM	121.22	109.53	0.294	0.214	0.999	0.998
MM	108.54	101.52	0.215	0.185	0.998	0.999

MM: Mechanical mixture

Table 6: Raw characteristics of industry wastewater

Parameter	Value before adsorption	Value after adsorption		
		ZSM-5/AC	ZSM-5	MM
pH	1.5	5.1	6.1	6.5
Pb^{2+} (mg/L)	29.8	2.8	3.1	4.2
Cd^{2+} (mg/L)	18.1	3.7	4.1	5.1

MM: Mechanical mixture

ions, the decrease noticed was 12.84% and in the multiple metal ion system, 27.53% was noticed. The preferential uptake exhibited by the sorbents toward Pb^{2+} ions is due to smaller ionic radius and larger electronegativity compared to other co-cations. Similarly, Cd^{2+} ions also exhibited higher sorption capacity among the other investigated cations except Pb^{2+} ions. Compared to Pb^{2+} and Cd^{2+} ions, as evidenced from Table 7, Pb^{2+} ions exhibit higher sorption capacity and this might be due to smaller ionic radii and higher electro-negativity. Similar observations were reported earlier for the sorption of Pb^{2+} and Cu^{2+} ions by watermelon rind.

Desorption studies

Revival of the adsorbent is of essential significance for reducing the cost of the removal process. Desorption and regeneration potential of prepared adsorbents was studied using 0.1 M HCl as desorbing agent. 0.1 g of Pb^{2+} and Cd^{2+} loaded adsorbents were kept in contact with 20 mL of 0.1 M HCl for 30 min, and desorbed acidic solution was analyzed by atomic absorption spectrometry to determine the metal ion concentration. Desorption of Pb^{2+} and Cd^{2+} from the metal loaded activated carbons is presented in Table 9. It can be seen

Table 7: Effect of other bivalent metals on removal of Pb^{2+}

Sorption system	q_e (mg/g) ZSM 5-AC	% decrease in q_e ZSM-5/AC
Pb^{2+}	131.55	-
Pb^{2+}-Cd^{2+}	118.67	9.7
Pb^{2+}-Cu^{2+}	127.60	2.22
Pb^{2+}-Co^{2+}	128.97	0.33
Pb^{2+}-Zn^{2+}	127.56	0.15
Pb^{2+}-Cd^{2+}-Cu^{2+}-Co^{2+}-Zn^{2+}	118.45	8.99

Table 8: Effect of other bivalent metals on removal of Cd^{2+}

Sorption system	q_e (mg/g) ZSM 5-AC	% decrease in q_e ZSM-5/AC
Cd	121.24	-
Cd^{2+}-Pb^{2+}	105.67	12.84
Cd^{2+}-Cu^{2+}	118.78	2.02
Cd^{2+}-Co^{2+}	113.67	6.24
Cd^{2+}-Zn^{2+}	111.76	7.81
Cd^{2+}-Pb^{2+}-Cu^{2+}-Co^{2+}-Zn^{2+}	87.86	27.53

Table 9: Data on desorption for prepared adsorbents

Cycle No.	ZSM-5/AC		ZSM-5		MM	
	Pb^{2+}	Cd^{2+}	Pb^{2+}	Cd^{2+}	Pb^{2+}	Cd^{2+}
1	93.45	91.34	92.33	92.32	82.35	81.34
2	89.45	85.34	85.34	83.25	75.44	71.23
3	65.34	64.14	54.34	45.33	65.34	43.23

MM: Mechanical mixture

that the adsorbents can be effectively recycled for two cycles without affecting the efficiency. The adsorption efficiency is observed to reduce in the subsequent cycles.[27,28]

CONCLUSIONS

Zeolite with MFI structure ZSM-5 and its composite with activated carbon ZSM-5/AC have been prepared successfully by SADGC method, and their textural properties have been studied. The FTIR results confirm the presence of ring structures of silica and double 5 rings of crystalline ZSM-5. The XRD patterns of ZSM 5, ZSM-5/AC, and MM show the presence of crystalline peaks except for the activated carbon which was amorphous. The structural configuration of alumina atoms was investigated by Al MAS NMR. A pronounced peak at 56 ppm can be seen both in the ZSM-5 and ZSM-5/AC which corresponds to tetrahedral alumina species. The absence of a peak at 0 ppm demonstrates that alumina is entirely incorporated in the framework of both ZSM-5 and ZSM-5/AC. The SEM micrographs of ZSM-5/AC and ZSM-5 sample were taken, and except in AC in all other samples, crystalline zeolite particles were visible. BET analysis indicates the presence of both micropores and mesopores in both ZSM-5 and the composite. The results show that the prepared materials ZSM-5, ZSM-5/AC, and MM could efficiently remove around 100 mg/g of Pb^{2+} and Cd^{2+} from aqueous solution at an equilibrium time of 60 min. As a significant application, the modified adsorbents with the composite materials were tried out on an industrial effluent to check the capability of the adsorbents in the removal of Pb^{2+} and Cd^{2+}. It was observed that approximately 90% of the metal ions in question were removed by all the adsorbents tried out. The sorption capacity of the composite was tried in binary and multiple systems, and it was observed that the composite has a preferential adsorption over Pb^{2+} and Cd^{2+} in comparison with other bivalent metals. Desorption of Pb^{2+} and Cd^{2+} from the metal loaded composite materials resulted in 80–90% of Pb^{2+} and Cd^{2+} release for the first two cycles and showed marked decrease in the third cycle.

REFERENCES

1. Deshmukh R, Khardenavis AA, Purohit HJ. Diverse metabolic capacities of fungi for bioremediation. Indian J Microbiol 2016;56:247-64.
2. Singh V, Haque S, Niwas R, Srivastava A, Pasupuleti M, Tripathi CK, *et al.* Strategies for fermentation medium optimization: An in-depth review. Front Microbiol 2016;7:2087.
3. Sathiya M, Periyar S, Sasikalaveni A, Murugesan K, Kalaichelvan PT. Decolorization of textile dyes and their effluents using white rot fungi. Afr J Biotechnol 2007;6:424-9.
4. Asgher M, Bhatti HN, Ashraf M, Legge RL. Recent developments in biodegradation of industrial pollutants by white rot fungi and their enzyme system. Biodegradation 2008;19:771-83.
5. Valentín L, Feijoo G, Moreira MT, Lema JM. Biodegradation of polycyclic aromatic hydrocarbons in forest and salt marsh soils by whiterot fungi. Int Biodeterior Biodegradation 2006;58:15-21.
6. Kumaran NS, Dharani G. Decolourisation of textile dyes by white rot fungi *Phanerochaete chrysosporium* and *Pleurotus sajor-caju*. J Appl Technol Environ Sanit 2011;1:361-70.
7. Hassaan MA, Nemr AE. Health and environmental impacts of dyes: Mini review. Am J Environ Sci Eng 2017;1:64-7.
8. Tisma M, Zelic B, Racki DV. White-rot fungi in phenols, dyes and other xenobiotics treatment-a brief review. Croat J Food Sci Technol 2010;2:34-47.
9. Mckay G, Bino MJ, Altememi AR. External mass transfer during the adsorption of various pollutants onto activated carbon. Water Res 1986;20:435-42.
10. Mobasherpour I, Salahi E, Pazouki M. Removal of divalent cadmium cations by means of synthetic nano crystallite hydroxyapatite. Desalination 2011;266:142-8.
11. Mu GN, Tang LB. Adsorption of cd(II) ion and its complex compounds from solution on the surface of charcoal treated with an oxidation-negative ionizing method. J Colloid Interface Sci 2002;247:504-6.
12. Namasivayam C, Ranganathan K. Removal of arsenic (V) from aqueous solution using industrial solid waste: Adsorption rates and equilibrium studies. Environ Technol 1995;16:851-60.
13. Ouki SK, Kavanagh M. Performance of natural zeolites

for the treatment of mixed metal-contaminated effluents. Waste Manage Res 1997;15:383-94.

14. Ozer A, Pirinççi HB. The adsorption of cd(II) ions on sulphuric acid-treated wheat bran. J Hazard Mater 2006;137:849-55.

15. Park M, Choi CL, Lim WT, Kim MC, Choi J, Heo NH. Molten-salt method for the synthesis of zeolitic materials. I. Zeolite formation in alkaline molten-salt system. Microporous Mesoporous Mater 2000;37:81-9.

16. Perić J, Trgo M, Medvidović NV. Removal of zinc, copper and lead by natural zeolite-a comparison of adsorption isotherms. Water Res 2004;38:1893-9.

17. Poon CP. Removal of cadmium from wastewaters. Experientia 1984;40:127-36.

18. Querol X, Alastuey A, Lo'pez-Soler A, Plana F, Andre's JM, Juan R, et al. A fast method for recycling fly ash: Microwave-assisted zeolite synthesis. Environ Sci Technol 1997;31:2527-33.

19. Querol X, Moreno N, Umana JC, Alastuey A, Hernandez E, Lopez-Soler A, et al. Synthesis of zeolites from coal fly ash: An overview. Int J Coal Geol 2002;50:413-23.

20. Ramos RL, Mendez JR, Baron JM, Rubio LF, Coronado RM. Adsorption of Cd (II) from aqueous solutions onto activated carbon. Water Sci Technol 1997;35:205-11.

21. Rengaraj S, Yeon KH, Kang SY, Lee JU, Kim KW, Moon SH, et al. Studies on adsorptive removal of co(II),

cr(III) and ni(II) by IRN77 cation-exchange resin. J Hazard Mater 2002;92:185-98.

22. Scott J, Guang D, Naeramitmarnsuk K, Thabuot M, Amal R. Zeolite synthesis from coal fly ash for the removal of lead ions from aqueous solution. J Chem Technol Biot 2002;77:63-9.

23. Shaheen SM. Sorption and availability of cadmium and lead in different soils from Egypt and Greece. Geoderma 2009;153:61-8.

24. Shawabkeh RA. Adsorption of chromium ions from aqueous solution by using activated carbo-aluminosilicate material from oil shale. J Colloid Interface Sci 2006;299:530-6.

25. Shigemoto N, Hayashi H, Miyaura K. Selective formation of Na-X, zeolite from coal fly ash by fusion with sodium hydroxide prior to hydrothermal reaction. J Mater Sci 1993;28:4781-6.

26. Stani T, Dakovic A, Zivanovic A, Tomasevic-Canovic M, Dondur V, Milicevic S. Adsorption of arsenic (V) by iron (III)-modified natural zeolitic tuff. Environ Chem Lett 2009;7:161-6.

27. Suyama Y, Katayama K, Meguro M. NH4þ-adsorption characteristics of zeolites synthesized from fly ash. J Chem Soc Jpn 1996;1996:136-40.

28. Tamura C, Yao Z, Kusano F, Matsuda M, Miyake M. Conversion of waste incineration fly ash into al-substituted tobermorite by hydrothermal treatment. J Ceram Soc Jpn 2000;108:150-5.